Journal of Analytical Toxicology, 2017;1–10
doi: 10.1093/jat/bkx058
Article

Article

Identification of MT-45 Metabolites: *In Silico* Prediction, *In Vitro* Incubation with Rat Hepatocytes and *In Vivo* Confirmation

Camilla Montesano[1], Gabriele Vannutelli[1], Federico Fanti[1], Flaminia Vincenti[1], Adolfo Gregori[2], Anna Rita Togna[3], Isabella Canazza[4], Matteo Marti[4], and Manuel Sergi[5]

[1]Department of Chemistry, Sapienza University of Rome, Piazzale Aldo Moro 5, 00185 Rome, Italy, [2]Department of Scientific Investigation (RIS), Carabinieri, Viale di Tor di Quinto, 151, 00191 Rome, Italy, [3]Department of Physiology and Pharmacology Vittorio Erspamer, Sapienza University of Rome, Piazzale Aldo Moro 5, 00185 Rome, Italy, [4]Department of Life Sciences and Biotechnology (SVeB), University of Ferrara, Via L. Borsari 46, 44100 Ferrara, Italy, and [5]Faculty of Bioscience and Technology for Food, Agriculture and Environment, University of Teramo, Via Balzarini 1, 64100 Teramo, Italy

*Author to whom correspondence should be addressed. Email: msergi@unite.it

Abstract

MT-45 is a synthetic opioid with a pharmacological activity comparable to morphine and it has been involved in intoxications and fatalities reported in Europe and in USA. It was recently subject to control measures, but to date the metabolic pathways of the substance are still unknown. Using rat hepatocytes and LC–HRMS, 14 novel Phase I and II MT-45 metabolites were identified, products of monohydroxylation, dihydroxylation and N-dealkylation; glucuronide conjugation of mono- and dihydroxylated metabolites also occurred. The detected metabolites were firstly predicted *in silico*, then incubation of the drug with rat hepatocytes was carried out and the obtained metabolites were identified by LC–HRMS, with retention times, mass shift between theoretical mass and observed mass (<5 ppm), peak abundance and fragmentation pattern. Hydroxylated MT-45 was found to be the major metabolite of MT-45 *in vitro* experiments. The presence of all metabolites was confirmed by *in vivo* experiments in urine samples of CD-1 male mice; in these samples hydroxy-MT-45-glucuronide and di-hydroxy-MT-45-glucuronide are the most abundant metabolites, while the parent drug is found at concentration <10 ng mL^{-1} after 300 min. The knowledge of Phase I and II MT-45 metabolite structure is then crucial to develop analytical methods to identify MT-45 consumption in clinical and forensic testing.

Introduction

The so-called new psychoactive substances (NPS) do not represent a novelty in the drug market anymore, in fact the phenomenon has been largely reported and monitored worldwide since the late 1990s (1). Several progresses were made to manage the issues arising from the diffusion of the new drugs, efficient and innovative legal responses have been provided by different nations with the European Union in first line. In Europe, the European Monitoring Centre for Drugs and Drug Addiction (EMCDDA) has a central role in monitoring NPS and in providing information and risk-assessment reports on new drugs in accordance with Article 6 of Council Decision 2005/387/JHA (2). However, the speed at which NPS suppliers offer new alternatives is still a major concern for both legislators and analysts. From an analytical point of view, the most effective tool to face the NPS emergency is the use of sensitive and selective techniques such as high resolution mass spectrometry (HRMS) (3). By enabling accurate mass determination at high resolving

power, HRMS may be used to identify the exact mass of a molecule and its fragments, allowing the confirmation, or even the identification of a new substance, overcoming the limitations of multi-target screening (4). In practice, however, untargeted screening is not an easy task, especially when complex samples, such as biological matrices, are involved; newly introduced NPS still represent a challenge since analytical standards are not available, they are not included in commercial or in-house libraries and metabolic pathways are unknown.

MT-45 (1-cyclohexyl-4-(1,2-diphenylethyl)piperazine), a drug which was firstly developed in the early 1970s by the Japanese company Dainippon Pharmaceutical Co. Ltd, is a new abused synthetic opioid, with an analgesic activity comparable to morphine but with a higher toxicity in animals (5). MT-45 has been raising health concerns worldwide after serious harmful effects, comprising intoxications and fatalities, were reported in Europe (28 deaths have been associated with MT-45 in Sweden alone) (5) and in the United States (6, 7) over a short period of time; it was the 10th new psychoactive substance to be risk assessed by EMCDDA. As a result of the risk-assessment conclusions, which reported the toxicity as well as the dependence potential of the substance, MT-45 was recently subject to control measures across the Member States (Council implementing decision (EU) 2015/1873); however, up to date the metabolic pathways of the substance are still unknown (7).

The aim of this work was to ascertain the chemical structures of the metabolites of MT-45, in order to allow further pharmacological studies and to better assess the health implications of the abuse of this substance. In addition, the identification of the most abundant metabolites is of the utmost importance for developing analytical methods for clinical and forensic investigations (8). In fact, when metabolism is unknown, the determination of target analytes is critical; the few reports of MT-45 in biological fluids are mainly related to blood specimens where the unchanged compound may be detected in considerable amounts (6). MT-45 was detected in unchanged form also in urine samples from intoxicated patients (9).

The present study involved a classic approach comprising both *in silico* and *in vitro* experiments. Similar approaches were used to identify the metabolites of several NPS such as α-PVP, 2-DPMP, 3,4-DMMC and MPA (10), 4-methoxy-α-PVP (11), PV8 (12), AH-7921 (13), JWH-015, JWH-098, JWH-251, JWH-307 (14), ADB-FUBINACA, AB-FUBINACA, AB-PINACA, QUPIC, 5 F-QUPIC (15) and AKB-48 (16). In this study, the most abundant metabolites were firstly predicted *in silico*, incubation of the drug with rat hepatocytes was then carried out and the obtained metabolites were identified by LC–HRMS. As further confirmation, *in vivo* experiments were performed; several urine samples of CD-1 male mice in which MT-45 (6 mg/kg, i.p.) were administered, were analyzed. The usefulness of *in vivo* experiments, to confirm *in vitro* studies, was previously showed (13, 17). To compare the *in vivo* effect of MT-45 with the presence of its urine metabolites, behavioral tests (mechanical analgesia and breath rate analysis) were performed in CD-1 male mice. Moreover, in order to better understand the *in vivo* efficacy of MT-45, morphine was used as reference compound.

To the best of our knowledge, this is the first study to report the metabolic profile of MT-45. Urine drug clearance data for MT-45 in mouse are also provided.

Materials and Methods

Chemicals and reagents

MT-45, cocaine and morphine were obtained by LGC standard (Sesto San Giovanni, Milan, Italy). MT-45 for *in vitro* and *in vivo* experiments was purchased from Composynth Chemicals (Mississauga, ON, Canada) and it was analyzed, to confirm its identity and purity (>95%), using the presented HPLC–MS-MS by comparison with the standard. Pooled cryopreserved male rat (Sprague-Dawley) hepatocytes, Williams' E Medium (phenol red free), cell maintenance supplement pack (Dexamethasone, Cocktail B: penicillin-streptomycin, ITS + (insulin, transferrin, selenium complex, BSA and linoleic acid), GlutaMAX™ and HEPES), as well as thawing and plating supplement pack (Prequalified fetal bovine serum (FBS), Dexamethasone, Cocktail A: FBS, penicillin-streptomycin, human recombinant insulin, GlutaMAX™ and HEPES) were purchased from Life Technologies (Monza, Italy).

Formic acid, methanol, acetonitrile and water were purchased from Fisher Scientific (Fair Lawn, NJ, USA). All solvents employed in the incubation were ultra-performance liquid chromatography (UHPLC) grade, and LC–MS grade in the chromatographic system. For *in vivo* studies, drugs were dissolved in saline solution (0.9% NaCl) and administrated intraperitoneally at a volume of 4 μL g^{-1}; saline solution was also used as the vehicle. Dose of morphine and MT-45 (6 mg kg^{-1} i.p.) was chosen based on preliminary studies (unpublished data).

In silico prediction study

Metaprint2D Freeware (S. Adams, Centre for Molecular Science Information, University of Cambridge) was used for *in silico* prediction of MT-45 metabolites. The structure of MT-45 was imported as SMILE code and predictions were generated using rat liver model. The most probable sites and relative reactions were estimated based on the NOR, a probability score assigned by Metaprint2D; a high NOR indicated, a more frequently reported site of metabolism in the metabolite database.

The chosen sites had a NOR score between 1 and 0.15. The predicted metabolites were reimported as SMILE code to predict Phase II metabolites with highest NOR score. SMILE code was generated using Marvin Sketch (v. 16.6.13.0, ChemAxon Ltd).

Rat hepatocyte incubation

For *in vitro* incubation experiments, MT-45 (20 μmol L^{-1}) was incubated at 37°C with rat cryopreserved hepatocytes. Cells were thawed in and washed with Williams' E Medium, containing dexamethasone (1 μM), penicillin/streptomycin (1%), human recombinant insulin (4 μg mL^{-1}), Glutamax™ (2 mM), Hepes pH 7.4 (15 mM) and FBS (5%) and centrifuged at 55×g for 3 min at room temperature. After centrifugation and removal of the supernatant, the cell pellet was resuspended in Williams' E Medium, containing dexamethasone (0.1 μM), penicillin/streptomycin (0.5%), human recombinant insulin (6.25 μg mL^{-1}), human transferrin (6.25 μg mL^{-1}), selenous acid (6.25 ng mL^{-1}), BSA 1.25 mg mL^{-1}, linoleic acid (5.35 μg mL^{-1}), Glutamax™ (2 mM) and Hepes pH 7.4 (15 mM) Cell viability was assessed with the Trypan blue 0.4% exclusion method.

About 10 μL of MT-45 1 mM was incubated in 500 μL of a 1.10^6 cell mL^{-1} suspension, at 37°C in a water bath under constant gentle shaking. Cocaine was also incubated, as a positive control, to verify metabolic capability under our experimental conditions. Samples were collected at 0.5, 1, 2 and 3 h; reaction was quenched by adding 500 μL acetonitrile. Specimens were stored at −20°C until analysis.

Before injection, samples were centrifuged; the supernatant was removed, diluted 1:2 with water and filtered with Minisart SRP25 4 mm (0.45 μm) syringe filters (Sartorius, Turin, Italy).

In vivo studies

Animals

The Male ICR (CD-1®) mice, 25–30 g (Harlan Italy; S. Pietro al Natisone, Italy) were group-housed (8–10 mice per cage; floor area per animal was 80 cm^2; minimum enclosure height was 12 cm) in a colony room under constant temperature (20–22°C) and humidity (45–55%). Food (Diet 4RF25 GLP, Milan, Italy) and tap water were available ad libitum all the time the animals spent in their home cages. The daylight cycle was maintained artificially (dark between 6 p.m.–6 a.m.). Experiments were performed during the light phase and each mouse was used for only one experiment. Experimental protocols performed in the present study were in accordance with the new European Communities Council Directive of September 2010 (2010/63/EU) a revision of the Directive 86/609/EEC, and were approved by the Italian Ministry of Health (license n. 335/2016-PR) and by the Ethics Committee of the University of Ferrara. Moreover, adequate measures were taken to minimize the number of animals used and their pain and discomfort. About 6 mice were used in experiment for urine collection, while 16 mice (8 for MT-45 and 8 for morphine evaluation) were used for acute mechanical nociception and breath rate evaluation.

Urine collection and sample preparation

Urine was collected by placing each mouse in a cage with a plastic grid in the floor that allows the recovery of urine. As soon as the urine of mice was deposited under the grid, it was immediately collected and pipetted into sterilized vials that were stored at −20°C. The time at which the urine was collected is recorded. The day of experiment at least 200 μL of urine were collected for each mouse (internal control sample) before MT-45 administration at 6 mg kg^{-1} i.p.

Before injection, urine samples were diluted 1:4 with methanol and filtered with Minisart SRP25 4 mm (0.45 μm) syringe filters (Sartorius, Turin, Italy).

Evaluation of pain induced by a mechanical stimulus

Acute mechanical nociception was evaluated using the tail pinch test (18). Pinch pressure was applied to the third of the tail extending from the root via a special rigid probe connected to a digital dynamometer (ZP-50 N, IMADA, Japan). Mice did not vocalize during the application of tail pinch pressure and when the mouse flicked its tail, the pressure was stopped and the digital instrument saved the maximum peak of weight supported (g $force^{-1}$). A cut off (500 g $force^{-1}$) was set to avoid tissue damage. The test was repeated 3 times and the final value was calculated with the average of 3 obtained scores. Acute mechanical nociception was measured at 0, 35, 55, 90, 145, 205, 265 and 325 min post injection.

Evaluation of breath rate

The experimental protocol for the detection of respiratory parameter in this study provides for monitoring of the animal awake, freely moving, with a non-invasive and minimal handling.

The animal is leaving free in a cage and the respiration patterns of the mice were videotaped by a camera (B/W USB Camera day&-night with varifocal lens; Ugo Basile, Italy) placed above the observation's cage. A trained operator who does not know the drug treatments performed analyzes movies off-line. The analysis frame by frame allows to better evaluate the number of breath rates of the mouse evaluated through the count of abdomen movement. Basal respiratory rates in mice was of about 257 ± 11 breath rates per minutes (brp). Breath rates were measured at 0, 10, 35, 65, 85, 125, 185, 245 and 305 min post injection.

Data and statistical analysis

Data are expressed in percentage of baseline (breath rates) and in percent of maximal possible effect {EMax% = [(test − control latency)/(cut off time − control)] × 100} in the tail pinch test. Statistical analysis was performed by two-way ANOVA followed by the Bonferroni's test for multiple comparisons for the analysis of the dose response curve of each compounds at different times (Panel A, B). We performed the statistical analysis on the average responses obtained, at each time point and dose compared. The statistical analysis was executed by means of the Prism software (GraphPad, San Diego, CA, USA).

LC–HRMS metabolite profiling

HPLC-HRMS analysis was carried out on a Thermo Scientific Ultimate 3000 RSLC system coupled to a Thermo Scientific Q-Exactive Mass spectrometer (Thermo Fisher Scientific, Bremen, Germany).

The column used for chromatographic separation was a C18-PFP (100 × 3 mm ID) from Ace (Aberdeen, Scotland) packed with particles of 3 μm, held at 40°C at a flow rate of 0.6 mL min^{-1}. Mobile phases were: 0.1% formic acid in water (Phase A) and 0.1% formic acid in acetonitrile (Phase B). The initial composition (5% B) was increased from 5% to 50% B over 4.5 min, from 50% to 100% over 0.5 min, held at 100% for 2 min and returned to initial conditions over 1 min. A 2 min equilibration followed, yielding a total run time of 10 min. The injection volume was 6 μL.

The Q-Exactive mass spectrometer was equipped with a heated electrospray ionization source (HESI-II) operated in positive mode. The operating parameters of the ion source were set as follows: spray voltage 3.5 kV, capillary temperature 350°C, heater temperature 450°C, S-lens RF level 60, sheath gas flow rate 55, auxiliary gas flow rate 20. Nitrogen was used for spray stabilization, for collision-induced dissociation experiments in the high energy collision dissociation (HCD) cell and as the damping gas in the C-trap. The instrument was calibrated in the positive and negative mode every working day. On every sample a full-scan acquisition, in the range of m/z 50–600, was carried out at a resolution of 35,000 (FWHM at m/z 450) in order to detect the metabolites predicted *in silico* as well as potential unpredicted metabolites. Automatic Gain Control (AGC) and maximum injection time were set at 1×10^5 and 50 ms, respectively.

For identification purposes, metabolite precursor ions, which were detected in full scan, were listed in an inclusion list in order to perform target MS/MS experiments. Precursors were filtered in the quadrupole with a 0.4 m/z isolation window and then fragmented in the HCD cell with different normalized collision energy (NCE) ranging from 20% to 55%. A scan of all the fragment ions was performed in the Orbitrap analyzer in the range of m/z 50–550. For these tests the MS/MS experiment performed in a separate run.

LC–MS-MS semi-quantitative method

The HPLC equipment consisted of a Series 200 Micro-LC Pump and a Series 200 autosampler from Perkin Elmer (Norwalk, CT,

USA). An API 2000 from AB-Sciex (Toronto, ON, Canada) equipped with a TurboIon-Spray source was used for analysis.

MT-45 and metabolites were separated using a reverse-phase F5 Kinetex column from Phenomenex packed with core shell particles (2.6 μm, 2.1 × 100 mm). A Phenomenex security GuardUltra Cartridge was also used to protect the column. The mobile phases were water (Phase A) and acetonitrile (Phase B) both containing 5 mM formic acid; the flow rate was 300 μL min^{-1} but only 100 μL min^{-1} were transferred to the ion source by means of a splitting system. The analyte separation was performed using a gradient elution according to the following steps: for 0.5 min Phase B is maintained at 0%, Phase B is then increased from 0 to 35% in 0.5 min, then to 60% in 4.5 min and to 100% in 1.5 min. Phase B is kept at 100% for 2 min; afterwards, the system is switched back to the initial conditions in 3 min. All the substances were detected in positive ionization (PI) with a capillary voltage of 5500 V, nebulizer gas (air) at 65 psi, turbo gas (nitrogen) at 35 psi and 425°C. The injection volume was 6 μL.

The optimum conditions for detection were determined with MT-45 and later used with slight modifications with metabolites. A MT-45 solution at 10 ng mL^{-1} in methanol was prepared for this purpose. Data collection and elaboration were performed by means of Analyst 1.5 software (PE Sciex). The chromatographic profiles were recorded by use of different MS(/MS) acquisition modes. SIM mode on Q1 was used to detect the metabolites previously identified in HRMS (m/z 365, 381, 169, 185, 541, 557) and to optimize the chromatographic conditions. Product-ion scan (PIS) experiments at different collision energies were carried out to confirm the data and to identify the optimal conditions for detection.

Finally, to obtain the maximum instrumental sensitivity, multiple reaction monitoring (MRM) acquisition was applied using the MS/MS information obtained from the previous runs. The selected masses, together with the main LC–MS/MS conditions, are reported in Table S1. This acquisition method was used to obtain pharmacokinetic data and to analyze urine samples.

Results and Discussion

In silico results

MetaPrint2D identified 9 potential Phase I metabolites of MT-45; the most probable metabolite, with NOR between 1 and 0.66, arose from the hydroxylation on the para position of the cyclohexane ring. According to the software, hydroxylation could occur also on the aromatic rings, leading to two additional hydroxylated metabolites, with a NOR between 0.33 and 0.15. A N-dealkylated metabolite was also predicted, with a NOR between 0.33 and 0.15.

Considering the high NOR scores (between 1 and 0.33) obtained for these metabolites, their structures were reintroduced in the software, leading to the identification of additional possible metabolites. A second hydroxylation on each cycle (cyclohexane or both aromatic rings) could lead to 3 dihydroxylated metabolites and hydroxylation was retained possible also for the N-dealkylated metabolite (on cyclohexane). A trihydroxylated metabolite (one hydroxylation on each cycle) was also predicted by the software. For Phase II metabolism prediction, Phase I metabolites were reintroduced in MetaPrint2D; according to the software the sole acceptable Phase II reaction was glucuronidation on hydroxylated sites.

Metabolites identification *in vitro*

Hepatocytes incubation allowed to mimic the physiological liver environment and to generate a realistic metabolic fingerprint of MT-45. The exploitation of *in silico* results enabled to detect and identify the major metabolites without using any software or data mining tools. Accurate masses were extracted from full-scan experiments and product-ion spectra were generated in tandem MS experiments. The structures of the observed metabolites were confirmed based on the observed retention times, mass shift between theoretical mass and observed mass (<5 ppm), peak abundance and fragmentation pattern.

Cocaine (positive control) and its metabolites, benzoylecgonine (BEG), norcocaine and ecgonine methyl ester (EME), were observed in the hepatocyte samples confirming hepatocyte metabolic activity.

Fourteen major MT-45 metabolites (10 Phase I and 4 Phase II) with mass measurements shifts <5 ppm were identified in the hepatocyte samples (Table I). Retention time was between 0.44 and 3.87 for metabolites while MT-45 eluted at 4.64 min. Consistent with ongoing metabolism, MT-45 peak area decreased during incubation while in general metabolite peak areas increased from 0.5 to 3 h (Figure 1). All 14 metabolites, especially Phase I, were identified in the 0.5 h sample, showing an extensive metabolism.

The metabolic reactions observed included: hydroxylation (M1, M2, M3), dihydroxylation (M4, M5, M6, M7, M8), N-dealkylation (M9), hydroxylation+N-dealkylation (M10); glucuronide conjugates

Table I. MT-45 metabolites identified after incubation with rat hepatocytes. Fragment ions are expressed in nominal mass

		Rt (min)	Elemental composition	m/z	Mass error (ppm)	Characteristic fragments
P	MT-45	4.64	C24H32N2	349.2634	−2.9	181, 166, 169, 103, 87
M1	hydroxy-MT-45 isomer 1	3.48	C24H32N2O	365.2577	−4.4	169, 197, 119, 91
M2	hydroxy-MT-45 isomer 2	3.76	C24H32N2O	365.2579	−3.7	197,181, 166, 119, 91
M3	hydroxy-MT-45 isomer 3	3.87	C24H32N2O	365.2577	−4.4	181, 169, 105, 197, 167, 347
M4	di-hydroxy-MT-45 isomer 1	2.65	C24H32N2O2	381.2537	−1.4	197, 119
M5	di-hydroxy-MT-45 isomer 2	2.80	C24H32N2O2	381.2533	−2.4	197, 119
M6	di-hydroxy-MT-45 isomer 3	2.93	C24H32N2O2	381.2527	−3.8	363, 169, 121
M7	di-hydroxy-MT-45 isomer 4	3.12	C24H32N2O2	381.2525	−4.5	105, 185, 363
M8	di-hydroxy-MT-45 isomer 5	3.23	C24H32N2O2	381.2529	−3.4	105, 185, 363
M9	1-cyclohexyl-piperazine	0.64	C10H20N2	169.1697	−4.8	87, 83
M10	hydroxy-(1-cyclohexyl-piperazine)	0.44	C10H20N2O	185.1639	−4.2	87
M11	hydroxy-MT-45-glucuronide isomer 1	2.65	C30H40N2O7	541.2899	−2.7	365, 197, 169
M12	hydroxy-MT-45-glucuronide isomer 2	2.83	C30H40N2O7	541.2898	−2.9	119, 197
M13	di-hydroxy-MT-45-glucuronide isomer 1	2.12	C30H40N2O8	557.2845	−3.25	169, 135, 213
M14	di-hydroxy-MT-45-glucuronide isomer 2	2.57	C30H40N2O8	557.2843	−3.5	213, 167, 195, 381

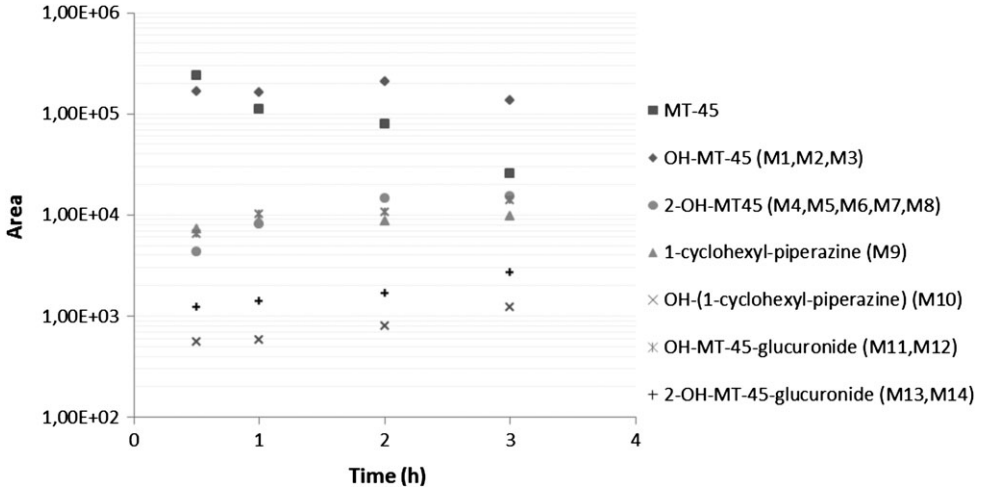

Figure 1. Peak areas of MT-45 and identified metabolites following rat hepatocytes incubation at 0.5, 1, 2 and 3 h.

were also observed (M10, M11, M12, M13). Compared to Phase I metabolites, glucuronide conjugates showed significantly lower areas. Based on observed peak areas, M1, M2, M3 were the most intense metabolites in hepatocyte incubation samples, followed by M9 and M4, M5, M6, M7, M8. These results were in accordance with the *in silico* prediction. However the trihydroxylated metabolite, predicted *in silico*, was not found *in vitro*. Hydroxylation on the aromatic ring was reported to be one of the initial metabolic step for structurally related 1,2-diphenylethylamines (19), supporting the obtained results.

In order to characterize the observed metabolites, target MS/MS experiments were performed at different NCE. A number of characteristic product ions were observed for MT-45 (Figure 2). The cleavage between the piperazine moiety and the diphenylethane led to the ions at m/z 181.1005 and 169.1695. The fragmentation between a phenyl and the ethane bridge generated the ion at m/z 103.0543. On the other hand the ion at m/z 166.0773, could be explained as a result of a rearrangement of the diphenylethane moiety for increased stability, and arose from the formation of alternating double bonds and loss of CH_3 as a radical. A similar fragmentation pattern was observed for structurally related 1,2-diphenylethylamines (19). Finally, the ion at m/z 87.0920 corresponded to the piperazine, resulting from the losses of both the cyclohexane and the diphenylethane moieties.

OH-MT-45 (M1, M2, M3), was the most intense metabolite in the hepatocyte samples. Three isomers, chromatographically separated, were observed in all the samples. The fragmentation pattern at different NCE are shown in Figure 3: the three isomers showed all the characteristic fragments of the precursor MT-45 but also a number of ions that suggested that a hydroxylation occurred on one of the aromatic ring. In fact the metabolic introduction of a hydroxy group into the diphenylethane moiety led to a shift of 16 u from the ion at m/z 181.1008 to m/z 197.0956 and from m/z 103.0542 to m/z 119.0491. These two ions were observed in the fragmentation pattern of the three isomers and were particularly abundant in M2 and M3. In M1 spectra at high NCE, the most abundant ion was at m/z 105.0336; accurate mass measurements confirmed that this ions corresponded to C_7H_50, showing that also for M1 the hydroxylation occurred on one of the aromatic ring.

M4, M5, M6, M7 and M8 are different positional isomers of di-OH-MT45. Five isomers of the ion at *m/z* 381 were observed; considering the poor chromatographic separation it was not possible to assign a structure to each peak, in particular M7 and M8 as well as M4 and M5, were not well resolved chromatographically and showed similar fragmentation patterns (Figure 4). Accurate mass measurements allowed to identify a number of characteristic fragments. The most intense ions in the spectra of M4 and M5 were 197.0957 and 119.0491, which suggested at least one hydroxylation on the diphenylethane moiety. M6 showed the fragments at *m/z* 363.2421, 169.1693 and 121.0286; this last exact mass corresponded to the formula $C_7H_5O_2$, which indicated that two hydroxylations occurred on the same aromatic ring. M7 and M8 characteristic fragments included *m/z* 105.0336, 185.1645 and 363.2412, which suggested that hydroxylations occurred on both the cyclohexane (185) and a phenyl (105) as already discussed by Lim *et al.* (20).

M9 and M10 were identified as (1-cyclohexyl-4-ethylpiperazine) and OH-(1-cyclohexyl-4-ethylpiperazine) and arose from the N-dealkylation of MT-45. Being quite hydrophilic they eluted early in the run (0.64 and 0.42 min, respectively), but it should be stressed that in the chromatographic conditions applied, the dead time of the column was < 0.2 min. Figure 5 illustrates the product-ion spectra for these metabolites. Only a few fragments could be observed, namely 87.0920 and 83.0859, which corresponded to the piperazine and the cyclohexane moieties.

M11, M12, M13 and M14 were Phase II metabolites. From the fragmentation pattern (Figure 6) it resulted that glucuronide conjugation always occurred on the aromatic ring. M11 and M12 are both mono-hydroxylated conjugates and they showed the fragment at *m/z* 197.0957 which resulted from the introduction of a hydroxy group into the diphenylethane moiety. On the other hand the bis-hydroxylated glucuronides, showed a number of characteristic fragments which implied that both hydroxy group were located on the aromatic rings. In fact, the fragment ion at *m/z* 213.0807, which was found in both spectra, arose from the shift of 16 u from the ion at *m/z* 197. Similarly, the ion at *m/z* 135.0438, which was observed in the spectrum of M13, corresponded to *m/z* 119 plus 16 u and provided evidence that two hydroxy groups were located on the same aromatic ring. M14 spectrum showed additional fragments, namely the ion at *m/z* 195.0801, which resulted from a loss of water from the ion at *m/z* 213, and the ion at *m/z* 167.0852 that may be explained by a loss of CO followed by a loss of water from the ion at *m/z* 213.

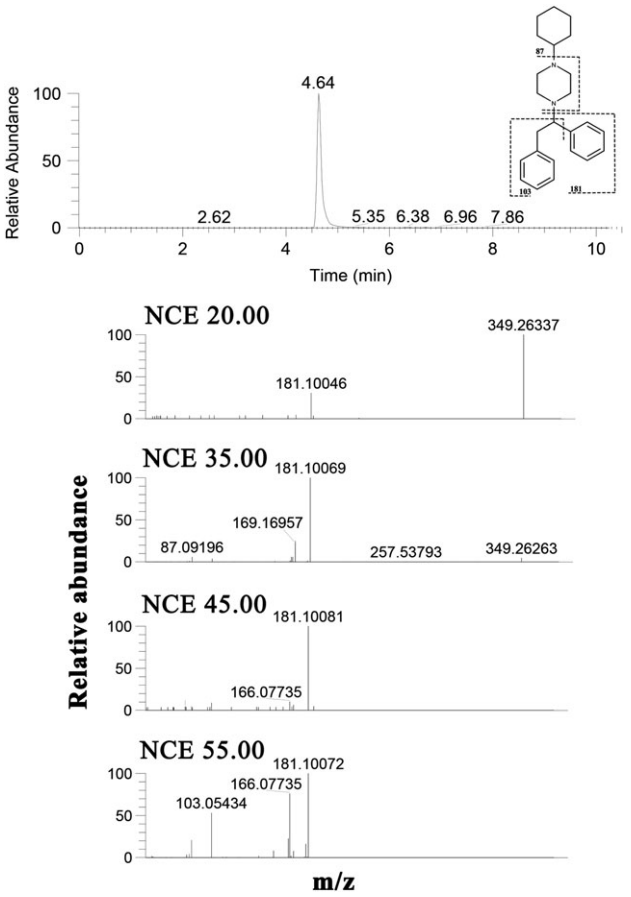

Figure 2. MS/MS spectra of MT-45 at different NCE and its fragmentation pattern.

Animal study: *in vivo* results

Urine analysis

The presence of all metabolites, identified during hepatocyte incubation, was confirmed in the urine specimens, highlighting the applicability of *in vitro* hepatocyte experiments for predicting *in vivo* metabolites. However we noticed that, in our experimental conditions, glucuronide conjugates were the most abundant metabolites in the urine specimens, while Phase I metabolites were the most abundant in the hepatocyte samples; M9 and M10, arising from N-dealkylation were more abundant in the authentic urine as well. However considering the different matrices, and the reduced clean-up for urine specimens (simple dilution) it must be considered that signal intensities also can be affected by different ionization efficiencies and matrix effects. The different intensities between *in vitro* and *in vivo* glucuronides conjugates peaks can also be explained as a consequence of glomerular filtration taking place in the nephron, in fact polar molecules are excreted more easily from blood stream, unlike the lipophilic molecules, which are reabsorbed and conjugated. This process does not perform during *in vitro* experiment.

The results, summarized in Figure 7, showed an extensive biotransformation of MT-45 *in vivo*, in all the animals MT-45 concentration rapidly decreased over time, to be lower than 10 ng mL^{-1} after 300 min. On the other hand at that time, metabolites are still in considerable amounts (for most metabolites area $>10^5$); the detection of MT-45 metabolites is thus essential to document MT-45 consumption during clinical and forensic urine testing. The results obtained show the need of synthesize MT-45 metabolites as reference standards for developing quantitative methods.

Urinary excretion patterns over time showed little inter-subject variability; N-dealkylated metabolites and OH-MT-45 decrease of over one order of magnitude after 300 min from MT-45 assumption. Di-OH-MT-45 and glucuronide conjugates decrease with a lower rate, showing a slower biotransformation. For most mice,

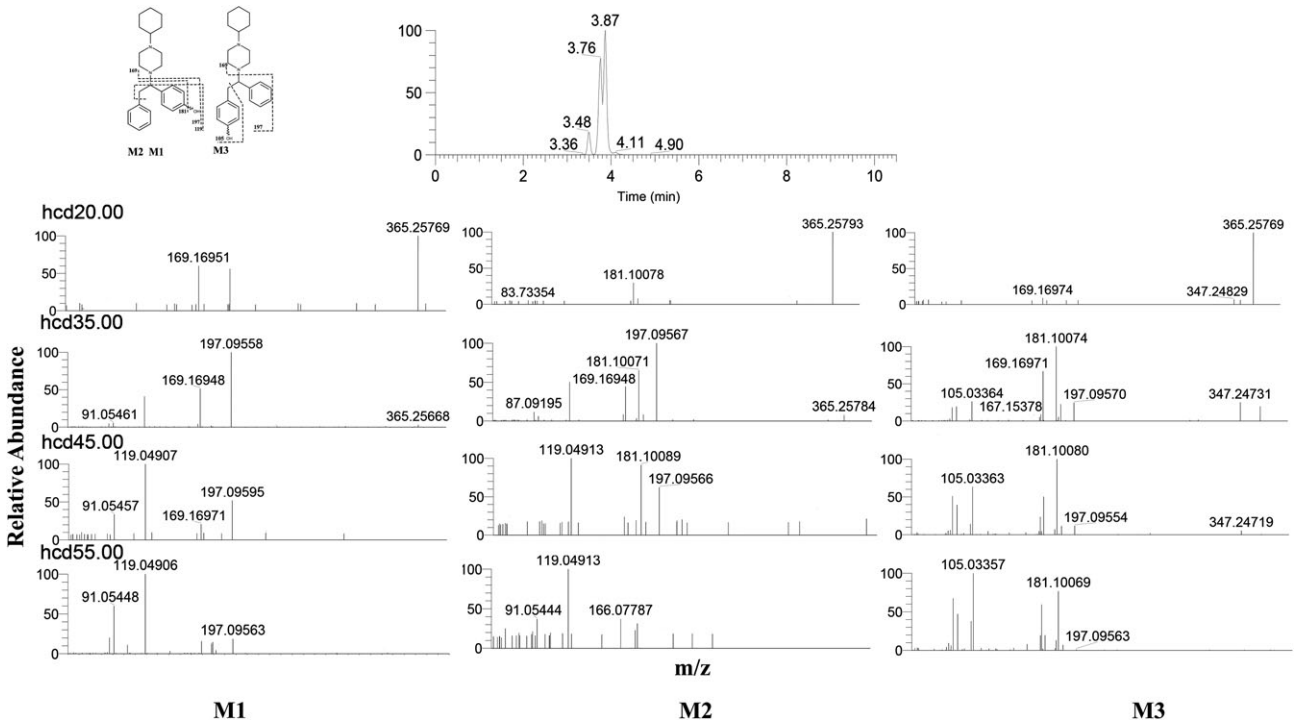

Figure 3. MS/MS spectra of MT-45 hydroxylated metabolites (M1, M2, M3) at different NCE.

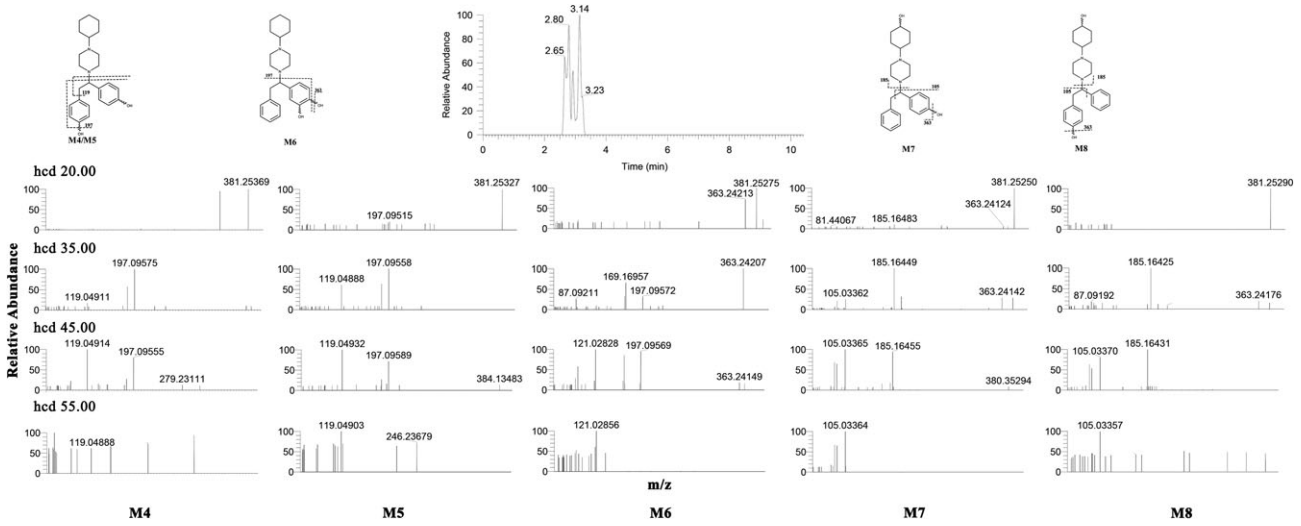

Figure 4. MS/MS spectra of MT-45 bis-hydroxylated metabolites (M4, M5, M6, M7, M8) at different NCE.

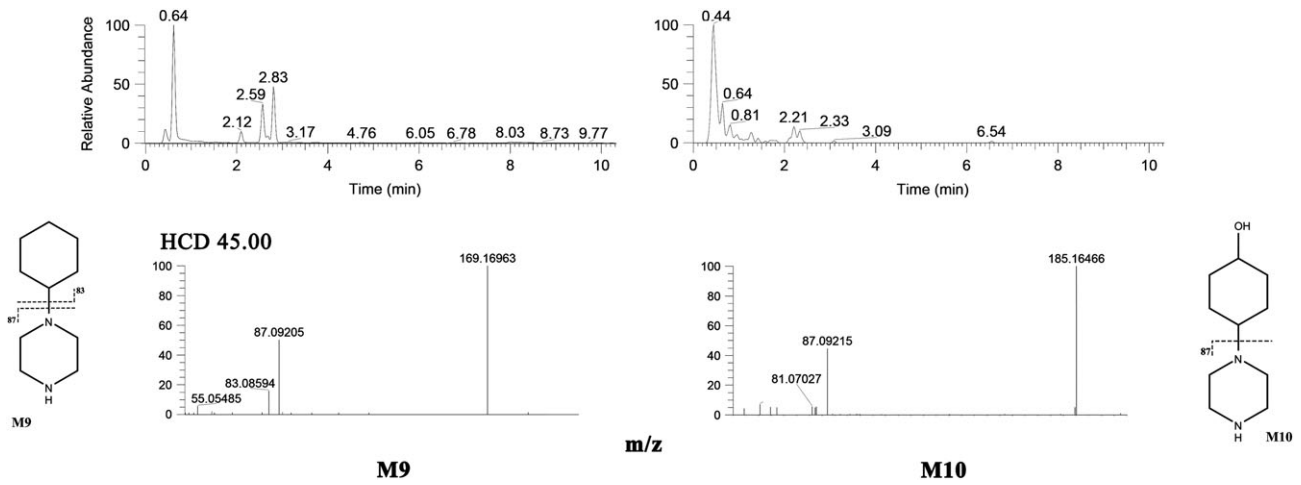

Figure 5. MS/MS spectra of MT-45 metabolites generated by N-dealkylation (M9, M10) at different NCE.

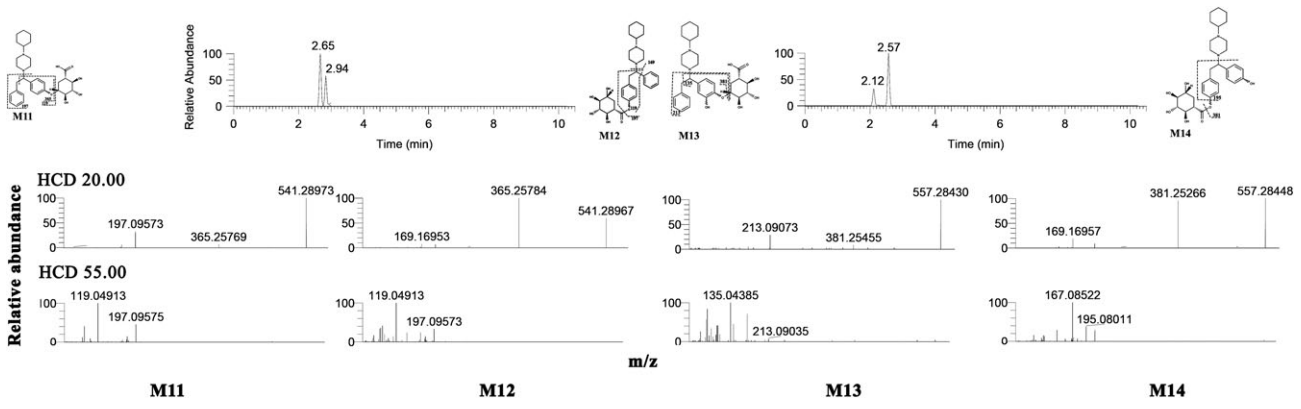

Figure 6. MS/MS spectra of MT-45 Phase II metabolites (M11, M12, M13, M14) at different NCE.

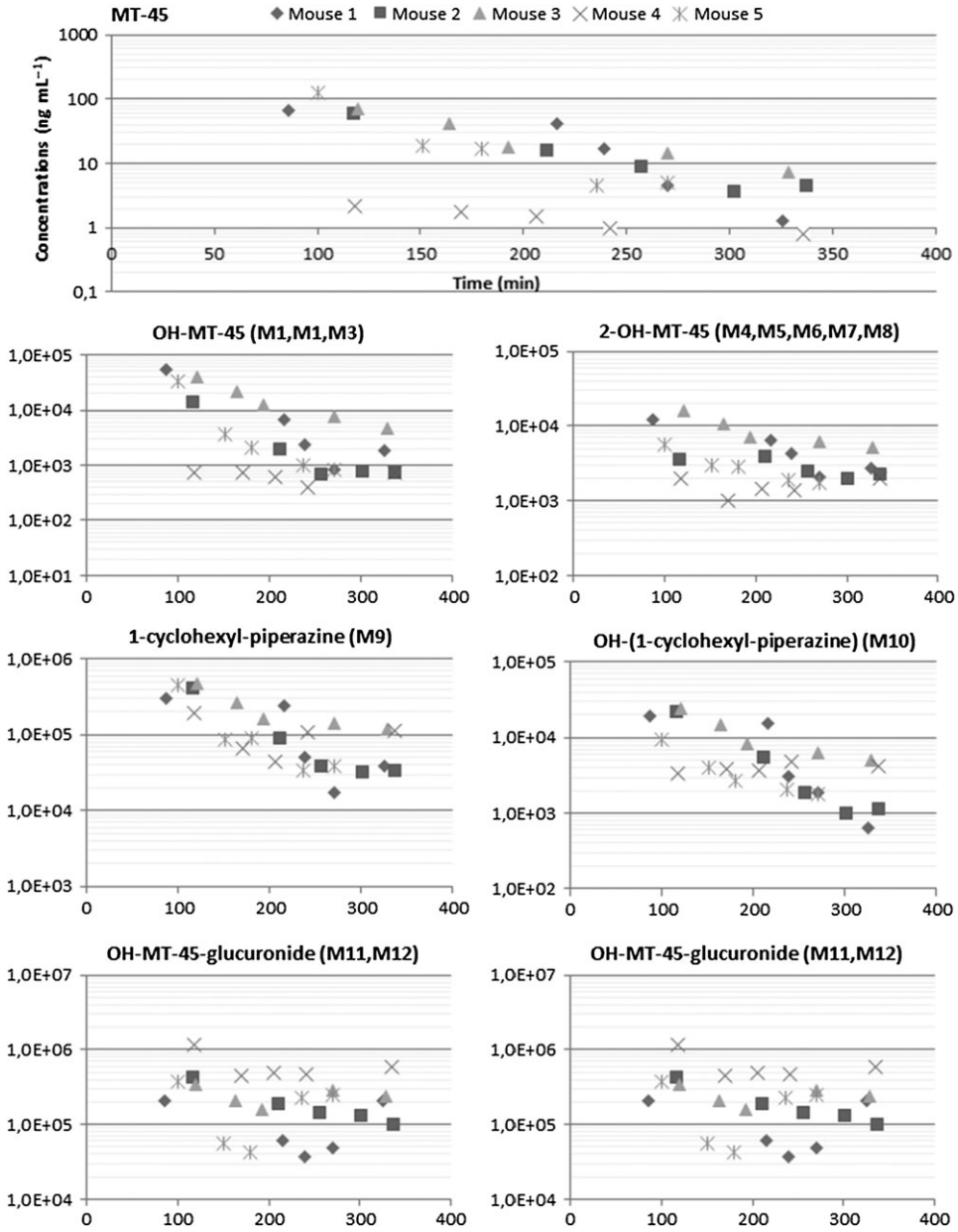

Figure 7. *In vivo* results: urinary concentration of MT-45 and peak areas of metabolites as a function of time after i.p administration of MT-45.

glucuronides display a double peak; a possible explanation for this behavior is that glucuronides are deconjugated and reabsorbed, or probably the different isoforms (M9-M13) are excreted at different times.

Behavioral studies

The threshold to acute mechanical pain stimulus in mice did not change in saline-treated mice over the 5 h observation (Figure 8 Panel A) and the response was similar to that observed in naïve untreated animals (data not shown). Systemic administration of MT-45 and morphine (6 mg kg^{-1} i.p.) increased the threshold to acute mechanical pain stimulus in mice in the tail pinch test (Figure 8 Panel A: significant effect of treatment ($F_{2,147} = 336.7$, $P < 0.0001$), time ($F_{6,147} = 27.90$, $P < 0.0001$) and time × treatment interaction ($F_{12,147} = 6.066$, $P < 0.0001$)). Both drugs show a similar profile, which is characterized by a maximum analgesic effect at 55 min (84.27% ± 4.34% and 91.24% ± 1.34%, respectively). After drug injection, analgesic effects were sustained and prolonged up to 205 min.

Respiratory rates did not change in saline-treated mice over the 5 h observation (Figure 8 Panel B) and the response was similar to that observed in naïve untreated animals (data not shown). Groups of mice treated with MT-45 and morphine have similar basal respiratory rates (274 ± 6 brp and 260 ± 6 brp, respectively). Systemic administration of MT-45 and morphine (6 mg kg^{-1} i.p.) reduced similarly the respiratory rates in a prolonged way just to 245 min after injection (Figure 8 Panel B: significant effect of treatment ($F_{2,168} = 48.83$, $P < 0.0001$), time ($F_{7,168} = 5.372$, $P < 0.0001$) and time × treatment interaction ($F_{14,168} = 1.960$, $P = 0.0237$)). The maximum effect was reached at 65 min for MT-45 (76.14% ± 5.26%) and at 125 min for morphine (82.50% ± 6.09%).

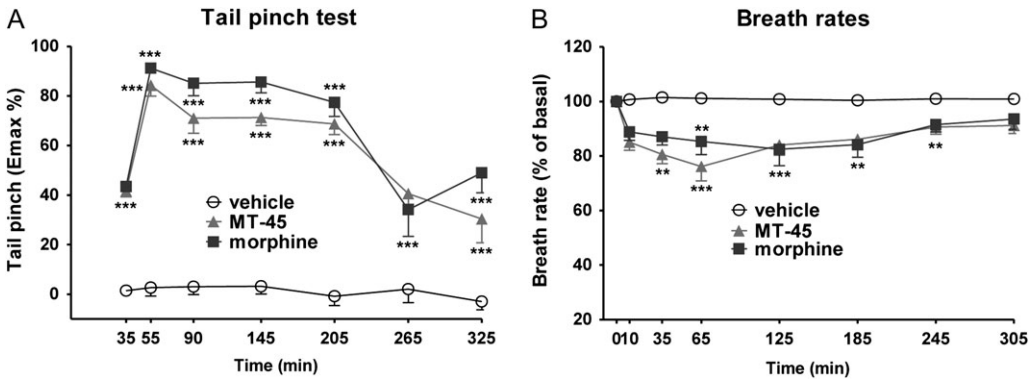

Figure 8. Effect of the systemic administration of MT-45 and morphine (6 mg kg^{-1} i.p.) on the tail pinch test (Panel A) and breath rates (Panel B) of mice. Data are expressed (see Material and Methods) as percentage of baseline (breath rates) and as percent of maximum effect (tail pinch test) and represent mean ± SEM of 8 animals for each treatment. Statistical analysis was performed by two-way ANOVA followed by the Bonferroni's test for multiple comparisons for both the dose response curve of each compound at different times (Panel A, B). $^{**}P < 0.01$, $^{***}P < 0.001$ versus vehicle.

Our behavioral data confirm that (racemic) MT-45 produces similar magnitude in mechanical analgesia and respiratory depression to morphine (21, 22) suggesting a similar potential for acute toxicity. Noteworthy, *in vivo* efficacy of MT-45 seems to overlap the pattern of the drug metabolism, suggesting that the acute pharmacological and toxicological activity of MT-45 could be mainly due to the "parent drug" instead of metabolites. However, further *in vivo* studies will be undertaken to better understand the profile of action of both MT-45 and its major metabolites.

Conclusions

In this work, the chemical structures of 14 Phase I and II MT-45 metabolites were identified using firstly the prediction *in silico*, then incubation of the drug with rat hepatocytes was carried out and the obtained metabolites were recognized by LC–HRMS. The detected metabolites were confirmed by *in vivo* experiments.

The structures of the observed metabolites were confirmed based on retention times, mass shift between theoretical mass and observed mass (<5 ppm), peak abundance and fragmentation pattern. It should be stressed that the relative amounts of metabolites were different between *in vivo* and *in vitro* experiments, with a prevalence of Phase II metabolites in real urine specimens while the opposite was found *in vitro* experiments.

The detected metabolites are mainly products of mono- or dihydroxylation, and N-dealkylation; glucuronide conjugation of mono- and dihydroxylated metabolites was also observed. Hydroxylated MT-45 demonstrated to be bioactive (23, 24) and may contribute to the overall pharmaco-toxicological profile of MT-45 *in vivo*.

The knowledge of Phase I and II MT-45 metabolite structure is also needed to develop analytical methods to identify MT-45 consumption in clinical and forensic testing.

Supplementary data

Supplementary data is available at *Journal of Analytical Toxicology* online.

Funding

Part of this research has been funded by the Drug Policies Department, Presidency of the Council of Ministers, Italy (project NS-Drugs to M. Marti), by local funds from the University of Ferrara (FAR 2016 to M. Marti)

References

1. King, L.A., Kicman, A.T. (2011) A brief history of 'new psychoactive substances'. *Drug Testing and Analysis*, **3**, 401–403.
2. Official Journal of the European Union. (2005) Council Decision 2005/387/JHA of 10 May 2005 on the information exchange, risk-assessment and control of new psychoactive substances. http://eur-lex.europa.eu/legal-content/EN/TXT/PDF/?uri=CELEX:32005D0387&from=EN (accessed Mar 2, 2017).
3. Favretto, D., Pascali, J.P., Tagliaro, F. (2013) New challenges and innovation in forensic toxicology: focus on the "New Psychoactive Substances". *Journal of chromatography. A*, **1287**, 84–95.
4. Montesano, C., Vannutelli, G., Gregori, A., Ripani, L., Compagnone, D., Curini, R., *et al.* (2016) Broad screening and identification of novel psychoactive substances in plasma by high-performance liquid chromatography-high-resolution mass spectrometry and post-run library matching. *Journal of Analitical Toxicology*, **40**, 519–528.
5. European Monitoring Centre for Drugs and Drugs Addiction. (2015) Report on the risk assessment of 1-cyclohexyl-4-(1,2-diphenylethyl)piperazine (MT-45) in the framework of the Council Decision on new psychoactive substances, Risk Assessments, Publications Office of the European Union, Luxembourg. http://www.emcdda.europa.eu/attachements.cfm/att_233323_EN_MT-45%20Risk%20Assessment%20Report.pdf (accessed Sep 12, 2016).
6. Papsun, D., Krywanczyk, A., Vose, J.C., Bundock, E.A., Logan, B.K. (2016) Analysis of MT-45, a novel synthetic opioid, in human whole blood by LC–MS-MS and its identification in a drug-related death. *Journal of Analytical Toxicology*, **40**, 313–317.
7. World Health Organization. (2015) MT-45 Critical Review Report Agenda item 5.1 Expert Committee on Drug Dependence Thirty-seventh Meeting Geneva, 16–20 November 2015. http://www.who.int/medicines/access/controlled-substances/5.1_MT-45_PR1.pdf?ua = 1 (accessed Jun 6, 2016).
8. Peters, F.T., Meyer, M.R. (2011) *In vitro* approaches to studying the metabolism of new psychoactive compounds. *Drug Testing and Analysis*, **3**, 483–495.
9. Helander, A., Backberg, M., Beck, O. (2014) MT-45, a new psychoactive substance associated with hearing loss and unconsciousness. *Clinical toxicology*, **52**, 901–904.
10. Tyrkko, E., Pelander, A., Ketola, R.A., Ojanperä, I. (2013) *In silico* and *in vitro* metabolism studies support identification of designer drugs in human urine by liquid chromatography/quadrupole-time-of-flight mass spectrometry. *Analytical and Bioanalytical Chemistry*, **405**, 6697–6709.
11. Ellefsen, K.N., Wohlfrath, A., Swortwood, M.J., Diao, X., Concheiro, M., Huestis, M.A. (2016) 4-Methoxy-alpha-PVP: *in silico* prediction, metabolic stability, and metabolite identification by human hepatocyte

incubation and high-resolution mass spectrometry. *Forensic Toxicology.*, **34**, 61–75.

12. Swortwood, M.J., Carlir, J., Ellefsen, K.N., Wohlfrath, A., Diao, X., Concheiro, M., *et al*. (2016) *In vitro*, *in vivo* and *in silico* metabolic profiling of -pyrrolidinopentiothiophenone, a novel thiophene stimulant. *Bioanalysis*, **8**, 65–82.
13. Wohlfarth, A., Scheidweiler, K.B., Pang, S., Zhu, M., Kronstrand, R., *et al*. (2016) Metabolic characterization of AH-7921, a synthetic opioid designer drug: *in vitro* metabolic stability assessment and metabolite identification, evaluation of *in silico* prediction, and *in vivo* confirmation. *Drug Testing and Analysis*, **8**, 779–791.
14. Strano-Rossi, S., Anzollotti, L., Dragoni, S., Pellegrino, R.M., Goracci, L., Pacali, V.L., *et al*. (2014) Metabolism of JWH-015, JWH-098, JWH-251, and JWH-307 *in silico* and *in vitro*: a pilot study for the detection of unknown synthetic cannabinoids metabolites. *Analytical and Bioanalytical Chemistry*, **406**, 3621–3636.
15. Takayama, T., Suzuki, M., Todoroki, K., Inoue, K., Min, J.Z., Kikura-Hanajiri, R., *et al*. (2014) UPLC/ESI-MS/MS-based determination of metabolism of several new illicit drugs, ADB-FUBINACA, AB-FUBINACA, AB-PINACA, QUPIC, 5F-QUPIC and alpha-PVT, by human liver microsome. *Biomedical Chromatography.*, **28**, 831–838.
16. Gandhi, A.S., Zhu, M., Pang, S., Wohlfrath, A., Scherdweiler, K.B., Liu, H., *et al*. (2013) First characterization of AKB-48 metabolism, a novel synthetic cannabinoid, using human hepatocytes and high-resolution mass spectrometry. *The American Association of Pharmaceutical Scientist Journal*, **15**, 1091–1098.
17. Caspar, A.T., Helfer, A.G., Michely, J.A., Auwarter, V., Brandt, S.D., Meyer, M.R., *et al*. (2015) Studies on the metabolism and toxicological detection of the new psychoactive designer drug 2-(4-iodo-2,5-dimethoxyphenyl)-N-[(2-methoxyphenyl)methyl]ethanamine (25I-NBOMe) in human and rat urine using GC-MS, LC-MS(n), and LC-HR-MS/MS. *Analytical and Bioanalytical Chemistry*, **407**, 6697–6719.
18. Vigolo, A., Ossato, A., Trappella, C., Vincenzi, F., Rimondo, C., Seri, C., *et al*. (2015) Novel halogenated derivates of JWH-018: behavioral and binding studies in mice. *Neuropharmacology*, **95**, 68–82.
19. Wink, C.S., Meyer, G.M., Wissenbach, D.K., Jacobsen-Bauer, A., Meyer, M.R., Maurer, H.H. (2014) Lefetamine-derived designer drugs N-ethyl-1,2-diphenylethylamine (NEDPA) and N-iso-propyl-1,2-diphenylethylamine (NPDPA): metabolism and detectability in rat urine using GC-MS, LC-MSn and LC-HR-MS/MS. *Drug Testing and Analysis*, **6**, 1038–1048.
20. Lim, T.C., Singh, R. (1991) Vibration transmission through rolling element bearings 0.3. geared rotor system studies. *Journal of Sound and Vibration*, **151**, 31–54.
21. Nakamura, H., Shimizu, M. (1976) Comparative study of 1-cyclohexyl-4-(1,2-diphenylethyl)-piperazine and its enantiomorphs on analgesic and othe pharmacological activities in experimental animals. *Archives Internationales De Pharmacodynamie Et De Therapie*, **221**, 105–121.
22. Fujimura, H., Tsurumi, K., Nozaki, M., Hori, M., Imai, E. (1978) Analgesic activity and opiate receptor binding of 1-cyclohexyl-4-(1,2-diphenylethyl)piperazine. *The Japanese Journal of Pharmacology*, **28**, 505–506.
23. Natsuka, K., Nakamura, H., Negoro, T., Uno, H., Nishimura, H. (1978) Studies on 1-substituted 4-(1,2-diphenylethyl)piperazine derivatives and their analgesic activities. 2. Structure-activity relationships of 1-cycloalkyl-4-(1,2-diphenylethyl)piperazines. *Journal of Medicinal Chemistry*, **21**, 1265–1269.
24. Nakamura, H., Ishii, K., Yokoyama, Y., Motoyosh, S., Natsuka, K., Shimizu, M. (1980) Analgesic and other pharmacological activities of a new narcotic antagonist analgesic (-)-1-(3-methyl-2-butenyl)-4-[2-(3-hydroxyphenyl)-1-phenylethyl]-piperazine and its enantiomorph in experimental animals. *Journal of Pharmacy and Pharmacology*, **32**, 635–642.